Mechanism of Hydrogen Transfer from Metal Hydrides

R. J. Klingler, K. Mochida, and J. K. Kochi*

Contribution from the Department of Chemistry, Indiana University, Bloomington, Indiana 47405. *Received March 7, 1979*

Abstract: The trialkyl metal hydrides of tin, germanium, and silicon (HMR_3) add spontaneously and selectively to olefins such as tetracyanoethylene (TCNE) to form characteristic 1:1 adducts, $H(TCNE)MR_3$. The metal hydride insertion shows no deuterium kinetic isotope effect and is not subject to radical-chain initiation or inhibition. The reactivity of the metal hydrides depends strongly on the metal, the second-order rate constant k_T decreasing in the order Sn > Ge > Si as $10^7:10^3:10^0$. The polar effect for alkyl substitution on tin hydride is obtained from a linear correlation with Taft σ^* values showing $\rho^* = -3$. A highly polar transition state is also indicated by the high sensitivity of the rate of n-Bu_3SnH reduction to solvent polarity. Furthermore, a linear correlation of rates (log k_T) with the reduction potentials $E°$ of TCNE and a series of quinones has a slope of 6.2, approaching the theoretical limit of 8.5 predicted by Marcus theory for complete outer-sphere electron transfer. Thus, the detection of transient charge-transfer complexes (HMR_3–TCNE) accords with an electron-transfer mechanism in which the metal hydride participates as an electron donor in the formation of the ion pair $HMR_3^+ \cdot TCNE^- \cdot$. The activation energy (E_T) for metal hydride insertion is a function of the ionization potentials of HMR_3, shown independently by photoelectron spectroscopy to increase in the order Sn < Ge < Si as 9.06:9.62:9.95 eV, in accord with the kinetic result. Most importantly, the same ion pair is produced by the direct irradiation of the charge-transfer band ($h\nu_{CT}$) at low temperatures, where the thermal electron transfer is too slow to compete. The charge-transfer complex is therefore common to the activation process for the photochemical ($h\nu_{CT}$) as well as the thermal (E_T) electron transfer. The insertion adducts are formed subsequently in a series of fast cage reactions involving the fragmentation of this metastable ion pair to a radical pair ($H \cdot MR_3^+TCNE^- \cdot$), in which the hydrogen atom and TCNE anion radical can be observed directly in a frozen matrix by their ESR spectra. The latter also allows the observation of the geminate combination of radicals to the insertion adduct H(TCNE)R. The selective insertion into the H–M rather than the R–M bond of R_3MH (despite a HOMO centered on the latter), is associated with the intimate nature of the ion pair derived by an inner-sphere mechanism for electron transfer comparable with that previously shown for the alkyl analogues R_4M. Finally, the use of deuterium kinetic isotope effects to probe hydrogen transfers by electron-transfer or hydride-transfer mechanisms is also considered in the more general light of dihydropyridine derivatives as hydride donors important in biological oxidation–reduction processes.

Introduction

Metal hydrides are common reagents for the reduction of a wide variety of organic functional groups.[1] Hydrido metal species are also involved as intermediates in a number of industrial catalytic processes, including the hydrogenation and hydroformylation of olefins.[2] However, despite their widespread involvement as reagents and intermediates, surprisingly little is quantitatively known about how the hydrogen–metal bond is broken and the hydrogen atom transferred, whether it be to an unsaturated C=C or C=O compound or even an organic halide.

Reductions with metal hydrides (MH) are often described as *hydride* transfers, simply on the basis of the regiospecificity of the transformation involved, e.g.,

$$MH + \rangle C{=}O \longrightarrow H{-}\overset{|}{\underset{|}{C}}{-}O{-}M$$

However, it is known that free-radical chain processes can also be involved.[3] Furthermore, hydrogen is an excellent σ-donor ligand, allowing metal hydrides to participate as electron donors.[4] Our approach to this problem is to delineate the structural factors involved in the reactivity of metal hydrides by first focussing on the extremes of the mechanistic spectrum. In this study we describe how charge-transfer interactions are basic to the reactivity of metal hydrides.

The group 4a metal hydrides of silicon, germanium, and tin were chosen since they are substitution stable and well behaved in solution to permit meaningful kinetic studies.[5] More importantly, the trialkyl derivatives R_3MH are sufficiently volatile for detailed photoelectron spectroscopic studies of the bonding orbitals (HOMO). These metal hydrides are known to add to a variety of unsaturated compounds, i.e.,

$$R_3MH + \rangle C{=}C\langle \longrightarrow R_3M{-}\overset{|}{C}{-}\overset{|}{C}{-}H$$

either spontaneously or after homolytic initiation.[6,7] The reactions of cyano-substituted olefin derivatives have been examined, but tetracyanoethylene (TCNE) is a particularly useful olefinic substrate since its physical and chemical properties are already well known.[8] We hope that the insight developed from establishing the mechanism of hydrogen transfer from a series of group 4a metal hydrides to tetracyanoethylene will provide a general framework for subsequent, more extensive studies of other metal hydrides (including those derived from the transition metals) with other organic functional groups.

Results

The reactivity of the alkyl derivatives of group 4a metal hydrides R_3MH toward tetracyanoethylene decreases in the order M = Sn > Ge > Si. Thus, triethylstannane reacts with TCNE on mixing, whereas the reaction with triethylsilane proceeds over several days at room temperatures.

Metal Hydride Adducts with TCNE. The product from the reaction of metal hydrides and TCNE is the 1:1 insertion adduct 1 (eq 1). However, 1 is labile and subject to further side

$$R_3MH + (NC)_2C{=}C(CN)_2 \longrightarrow R_3M{-}\overset{|}{C}(CN)_2{-}\overset{|}{C}(CN)_2H \qquad (1)$$

reactions, the severity of which is related to the solvent and to the metal as described below for two representative metal hydrides.

1. Trialkyltin Hydride. When trialkylstannane (R = Me, Et, n-Bu, and Ph) is added to an anhydrous solution of TCNE in acetonitrile, a mixture consisting of at least three products is formed. The principal product formed in ~90% yield is the 1:1 adduct showing a singlet resonance in the ^1H NMR spectrum for the unique hydrogen. Isolation of these adducts in pure form was complicated by the presence of tetracyanoethane (H_2TCNE) in ~10% yield and traces of paramagnetic impurities derived from TCNE anion radical. Rigorous purification and drying of the acetonitrile did not preclude H_2TCNE as an undesirable contaminant. Fortunately, the 1:1 adducts are insoluble in toluene and precipitate immediately in >80% yield when trialkylstannane is added to a toluene solution of

0002-7863/79/1501-6626$01.00/0

Table I. Spectral Characterization of Trialkylstannane and Adducts to TCNE

trialkylstannane			insertion adduct[a]			
R_3SnH	ν_{Sn-H},[b] cm^{-1}	δ_{SnH},[c] ppm	ν_{C-H}, cm^{-1}	$\nu_{C\equiv N}$, cm^{-1}	δ_H, ppm	δ_R, ppm
Me	1820	4.69	2990, 2910	2210, 2160	3.38 (s)	0.96 (s)
Et	1809	4.72	2970, 2950, 2920, 2870	2210, 2160	3.37 (s)	1.47 (m)
n-Bu	1807	4.67	2990, 2960, 2910, 2890	2210, 2160	3.40 (s)	1.25 (m) 0.80 (m)
i-Pr	1809	4.66				
Ph	1835	6.80			2.50 (s)	7.53 (m)

[a] Infrared spectra of adducts in Nujol and perfluoroalkane. ^1H NMR spectra in chloroform-*d* solvent, s = singlet, m = multiplet. [b] Neat liquid. [c] CD_3CN solution.

TCNE. The adduct after washing and reprecipitation is rather pure, judging from its complete elemental analysis. Analogous insertion adducts were prepared from various stannanes in Table I. The IR spectra are all completely free of any Sn—H absorptions (e.g., 1809 cm^{-1} in Et_3SnH), and the unique hydrogen in triethylstannane (δ 4.72, septet) is quantitatively shifted to a singlet resonance at δ 3.37 in the ^1H NMR spectrum of the TCNE adduct. The latter accords with the chemical shift for hydrogen bound to TCNE in the known alkane adducts R(TCNE)H, where R = Me, Et, and H.[9] However, barring an X-ray crystal structure (see Experimental Section), the attachment of the R_3Sn moiety is uncertain. The C≡N absorptions measured in acetonitrile solutions are an order of magnitude more intense than the corresponding values in the R(TCNE)H adduct, suggesting the possibility that tin is bound to nitrogen as in II rather than to carbon in III.

II

III

However, this assignment is not unequivocal since the ketenimine absorptions[10] usually observed between 1250 and 1400 cm^{-1} are absent in these adducts. In either case, the distinction between 1,4 and 1,2 adducts, II and III, respectively, is not so great as it may seem since these R_3Sn adducts are, substitutionally, quite labile (vide infra).

When pure, the 1:1 insertion adduct is rather stable in acetonitrile solutions. However, the addition of TCNE in even small amounts causes the clear, colorless solution to darken and eventually turn red (see Experimental Section). Similar development of highly colored solutions has been observed with polycyanoalkanes, and attributed to alkylation and condensation reactions with TCNE.[11] Hydrolysis of the 1:1 insertion adduct in acetonitrile solution afforded H_2TCNE in ~60% yield (eq 2).

$$R_3Sn(TCNE)H \xrightarrow{H_2O} H_2TCNE, \text{ etc.} \quad (2)$$

The chemical properties of the 1:1 insertion adducts of trialkylstannane were also examined. Thus, the tin hydride adducts to TCNE are moderately weak acids. Potentiometric titration of $Et_3Sn(TCNE)H$ with alkali in aqueous acetonitrile solution yields a titration curve which is similar to those obtained from $CH_3(TCNE)H$ and H(TCNE)H, with pK_a = 3.5 and 3.6, respectively, in water.[11,12]

The lability of the insertion adduct is also shown by its ready electrooxidation. Thus, cyclic voltammetry at a stationary platinum electrode exhibits a completely reversible oxidation at +0.229 volts relative to SCE as shown in Figure 1. The current function, $i_p\ V^{-1/2}\ C^{-1}$, which is proportional to the concentration of the electroactive species, is independent of the scan rate up to 200 mV s^{-1}. Significantly, it *decreases* with increasing concentration as shown in Table II. The latter suggests that the carbanion formed by acid dissociation is the electroactive form undergoing oxidation (eq 3 and 4). The

Table II. The Effect of Sweep Rate and Concentration on the Current Function during Cyclic Voltammetry of $Et_3Sn(TCNE)H$[a]

sweep rate, mV s^{-1}	$Et_3Sn(TCNE)H$, M	$i_p\ V^{-1/2}\ C^{-1}$, $\mu A\ mV^{-1/2}\ M^{-1}$
10	1.3	9.6
50	1.3	9.2
100	1.3	9.2
200	1.3	9.2
200	2.2	6.9
200	2.8	6.3
200	3.7	5.5
200	4.2	5.2

[a] In acetonitrile solution at 25 °C with platinum electrodes.

$$Et_3SnTCNEH \rightleftharpoons Et_3SnTCNE^- + H^+ \quad (3)$$

$$Et_3SnTCNE^- \underset{+e}{\overset{-e}{\rightleftharpoons}} Et_3SnTCNE\cdot \quad (4)$$

same effect is observed in the cyclic voltammogram of H_2TCNE, although the cathodic wave in this case is irreversible, owing to the reactivity of the radical (vide infra) (eq 5). The addition of small amounts of sodium acetate markedly

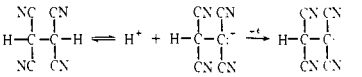

(5)

increases the current function in both cases, as expected.

Coulommetry accompanying the controlled potential oxidation of $Et_3Sn(TCNE)H$ in acetonitrile solution at 0.40 V releases 0.91 ± 0.05 electrons/mol of adduct. Cyclic voltammetry of the resultant solution exhibits only a reversible reduction at 0.229 V. Thus, the radical $Et_3SnTCNE\cdot$ is rather stable and reversibly formed in eq 4. The ESR spectrum of the solution taken after electrolysis shows the characteristic 9-line spectrum of a TCNE radical (g = 2.0030 and a_N = 1.53 G).[13-15] In the less polar 1,2-dichloropropane solvent, the ESR spectrum at low modulation amplitudes showed additional fine structure consisting of 45 lines (g = 2.0031; a_{N_1} = 1.21, a_{N_2} = 2.05, and $a_{N_{3,3}}$ = 1.75 G), which is assigned to the nitrogen-bound radical, IV. The radical species represented as IV,

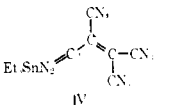

IV

however, is not a static structure since the relative intensities of the lines in the ESR spectrum do not accord with the expected distribution.[13] Selective line broadening is suggested which may be due to dynamic processes,[16] such as structural fluctuations in labile ion pairs (eq 6), which may alternately

$$Et_3SnTCNE\cdot \rightleftharpoons Et_3Sn^+\ TCNE^-, \text{ etc.} \quad (6)$$

bind tin to either the nitrogen or carbon center in the TCNE anion radical. Indeed, dynamic processes leading to line

Table III. Rate Constants for TCNE Insertion of Metal Hydrides[a]

metal hydride	M	ν_{CT},[b] cm^{-1}	temp, °C	TCNE, 10^5 M	k_T, M^{-1} s^{-1}
n-Bu_3SnH	$2.3-3.4 \times 10^{-4}$	15 400[a]	25	2.3	6.1×10^2
	8.2×10^{-3}	15 000[a]	25	6.5	6.9×10^2 [c]
n-Bu_3GeH	$1.4-8.1 \times 10^{-2}$	25 600	25	3.7	2.0×10^{-2}
	8.1×10^{-2}	25 600	35	3.7	3.8×10^{-2}
Et_3GeH	1.2×10^{-1}	24 400	25	3.7	1.7×10^{-2}
Et_3SiH	4.7×10^{-1}	34 500	34	4.8	3.3×10^{-5}
Et_4Ge[d]	1.4×10^{-1}	30 000	25	3.7	1.6×10^{-4}

[a] In acetonitrile solution. [b] Charge-transfer (CT) band in chloroform. [c] Determined by directly observing the decay of the CT band. [d] For comparison.

Table IV. Solvent Dependence of the Second-Order Rate Constant for Tin Hydride Insertion[a]

n-Bu_3SnH, 10^4 M[b]	TCNE, 10^5 M[b]	solvent	rate constant,[c] M^{-1} s^{-1}
0.81–14.8	1.16–25.3	cyclohexane	0.49 (20)
0.25–0.50	0.25–0.50	methylene chloride	160 (7)
2.30	2.1	ether	9.7 (2)
1.10–4.95	2.1	acetonitrile	612 (4)

[a] At 25 °C. [b] Range indicates k measured at various concentrations. [c] Number of determinations in parentheses.

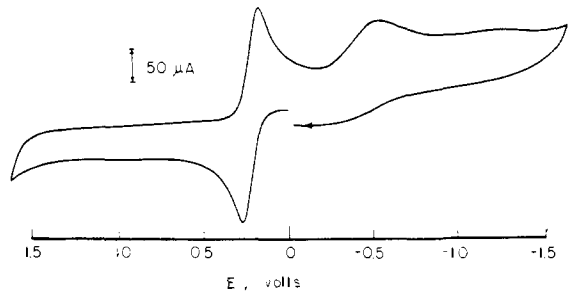

Figure 1. First-scan cyclic voltammogram of 1.3×10^{-3} M Et_3Sn(TCNE)H in acetonitrile containing 0.10 M tetraethylammonium perchlorate at a platinum microelectrode with a scan rate of 200 mV/s.

broadening can also be observed if radical IV is generated in the presence of unreacted TCNE. The intermolecular electron transfer rate k_{ex} can be estimated by the dependence of the ESR line width as a function of added TCNE in the fast exchange limit. The exchange rate of 2.6×10^9 M^{-1} s^{-1} calculated under these conditions is not much smaller than that (k_{ex} = 3.2×10^9 M^{-1} s^{-1}) reported for the self-exchange of the TCNE anion radical[17] itself (eq 7). Indeed, the remarkably

$$TCNE^{-\cdot} + TCNE \overset{k_{ex}}{\rightleftharpoons} TCNE + TCNE^{-\cdot} \quad (7)$$

similar values of the reversible reduction potential of $R_3SnTCNE\cdot$ ($E°$ = 0.229 V) and TCNE ($E°$ = 0.22 V) indicate that the disproportionation equilibrium in eq 8, is close to unity.

$$R_3SnTCNE^{-} + TCNE \overset{K_{disp}}{\rightleftharpoons} R_3SnTCNE^{+\cdot} + TCNE^{-\cdot} \quad (8)$$

2. Trialkylsilicon Hydride. TCNE insertion also takes place with trialkylsilanes, but the 1:1 adduct does not build up since it is formed too slowly to compete with facile side reactions. Thus, when triethylsilane is added to a solution of TCNE in acetonitrile, H_2TCNE and hexamethyldisiloxane can both be isolated in good yields after 2 days at room temperature. The expected 1:1 insertion adduct is the putative intermediate (eq 9), which undergoes ready hydrolysis with adventitious water

$$Et_3SiH + TCNE \longrightarrow Et_3SiOSiEt_3 \quad (9)$$

according to the stoichiometry in eq. 10. Moreover in the

$$2\,Et_3Si(TCNE)H + H_2O \longrightarrow 2\,H_2TCNE + Et_3SiOSiEt_3 \quad (10)$$

complete absence of water, the reactive silane adduct reacts with more TCNE, without forming H_2TCNE, to afford the red condensation product similar to that observed with the tin analogue I (vide supra). Under both conditions (i.e., in anhydrous and moist acetonitrile), the disappearance of Et_3SiH and TCNE occurs with the *same* second-order rate constant of 3×10^{-5} M^{-1} s^{-1}. Since the growth of H_2TCNE in moist acetonitrile also takes place at the same rate, it must occur via the rapid hydrolysis of the 1:1 adduct as in eq 10, subsequent to the rate-limiting insertion in eq 9.

The germanium analogues, Et_3GeH and *n*-Bu_3GeH, react with TCNE in essentially the same manner as that described for the silanes.

Reactivity Trends in TCNE Insertions with Tin Hydrides. To elucidate the mechanism of TCNE insertion into tin hydrides, we examined (1) the kinetics, (2) the deuterium kinetic isotope effect, (3) substituent effects on tin hydride reactivity, and (4) the effect of radical inhibitors. We also tested the possibility of (5) hydrogen transfer from tin hydrides to the $R_3SnTCNE\cdot$ radical as a step in the reaction.

1. Kinetics of Tin Hydride Insertion. The reaction between trialkyltin hydride and TCNE was followed spectrophotometrically by measuring the decrease in the absorbance of the strong π–π^* band of TCNE at 270 nm (ϵ 15 500 M^{-1} cm^{-1}). The kinetics of the reaction were determined by varying the relative concentrations of the reactants over a range encompassing 8×10^{-3} to 1.5×10^{-5} M for trialkyltin hydride and 1×10^{-5} to 2.5×10^{-4} M for TCNE. The rate showed a first-order dependence on each reactant (eq 11). The observed

$$-d[TCNE]/dt = k_T[R_3SnH][TCNE] \quad (11)$$

second-order rate constants k_T in Table III depend strongly on the metal, decreasing in the order Sn ≫ Ge > Si for analogous trialkylmetal hydrides.

The second-order rate constant for *n*-Bu_3SnH insertion is also strongly dependent on the solvent polarity. The latter is evaluated independently by the empirical solvent parameters, such as the Z and E_T* values.[18,19] For the solvents listed in Table IV, the polarity (measured as E_T* in kcal mol^{-1}) increases in the order cyclohexane (31), diethyl ether (35), methylene chloride (41), and acetonitrile (46).

2. Kinetic Isotope Effect. To ensure reliability, two independent measures of the deuterium kinetic isotope effect in tin hydride insertion were obtained. First, an equimolar mixture of *n*-Bu_3SnH and *n*-Bu_3SnD was treated with 0.1 equiv of TCNE. The change in stannane concentration was monitored

Table V. Competition Method for the Determination of the Kinetic Isotope Effect for Tin Hydride Insertion[a]

protio- or deuteriostannane[b]		TCNE,	stoichiometry[c]	
10^2 M_i	10^2 M_f	10^2 M		$\Delta_{SnH}{}^d/\Delta_{SnD}$
H 1.88	1.52	0.93	0.82	0.90
D 1.88	1.48	0.93		
H 1.88	1.42	1.08	0.89	0.92
D 1.88	1.38	1.08		

[a] Tri-*n*-butylstannane in cyclohexane solution at 25 °C. [b] M_i and M_f are initial and final concentrations, respectively. [c] $[\Delta_{SnH} + \Delta_{SnD}]$/TCNE. [d] Kinetic isotope effect determined by the change in *n*-Bu_3SnH and *n*-Bu_3SnD concentrations. Reliability is ±10%.

Table VI. Direct Method Determination of the Kinetic Isotope Effect for Tin Hydride Insertion in Various Solvents[a]

n-Bu_3SnH/D, 10^4 M	TCNE, 10^5 M	solvent	k_H/k_D[b]
3.78–12.6	2.31–4.63	cyclohexane	1.0 ± 0.1 (4)
0.25–0.50	0.25–0.50	methylene chloride	1.3 ± 0.1 (4)
2.30	2.10	ether	1.4 ± 0.1 (2)
1.10–4.95	2.10	acetonitrile	1.5 ± 0.1 (3)

[a] At 25 °C. [b] Number of determinations in parentheses.

by directly following the absorbances of the Sn–H and Sn–D IR bands at 1815 and 1280 cm^{-1}, respectively. Within experimental error (±10%), the combined decrease in stannane was equal to the amount of TCNE added as shown in Table V.

Alternatively, the absolute second-order rate constants for Sn–H and Sn–D insertion were measured separately by following the disappearance of TCNE spectrophotometrically. The kinetic isotope effects measured directly by this method in various solvents are listed in Table VI. The trend toward slightly higher values of k_H/k_D in the more polar solvents may be in part attributed to extraneous side reactions (vide supra) which are known to occur in these media.

We conclude, therefore, on the basis of competitive as well as direct measurements of rates, that TCNE insertion into metal hydrides proceeds with no perceptible, deuterium kinetic isotope effect.

3. Substituent Effects on Tin Hydride Reactivity. The effect of organic ligands on the reactivity of trialkyltin hydrides R_3MH varies substantially from R = Me, *n*-Bu, *i*-Pr, and Ph. The second-order rate constants listed in Table VII show no systematic electronic or steric effects. Thus, for the three trialkyl derivatives, the HOMO energies should decrease in the order Me > *n*-Bu > *i*-Pr in accord with the values of the ionization potentials listed in Table VIII.[20] The ionization potentials of the corresponding tetraalkyltin analogues, R_4Sn, are also included for comparison. Steric effects based on Taft E_s values[21,22] follow the opposite trend: R = Me < *n*-Bu < *i*-Pr. Furthermore, the Sn–H bond energies, though unmeasured, are expected to follow the trend Ph_3Sn–H < Me_3SnH < *i*-Pr_3SnH.

Inhibition Studies of Free-Radical Chain Processes. Galvinoxyl is known to be a highly effective inhibitor of the radical-chain addition of trialkyltin hydrides to various olefinic substrates.[7] However, galvinoxyl has no effect on the rate of the reaction between *n*-Bu_3SnH and TCNE when added in amounts up to 50% of the major reagent (see Figure 2). Control experiments show that galvinoxyl is stable to both stannane and TCNE, the amplitude of the ESR signal being unchanged in the period of the reaction. It is noteworthy, however, that galvinoxyl will react readily with the insertion adducts, as well as H_2TCNE. Thus, if the kinetics were simply based on the appearance of the adducts, the observation of an apparent inhibition would be misleading.

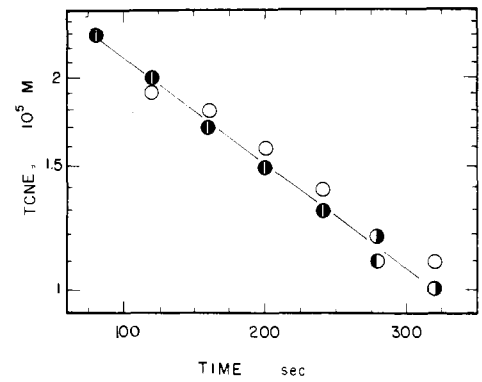

Figure 2. Effect of inhibitor on the insertion of 2.3×10^{-5} M TCNE and 6.0×10^{-3} M Bu_3SnH in acetonitrile at 25 °C. Galvinoxyl added: ●, none; ◑, 6.0×10^{-4} M; ○, 3.0×10^{-3} M.

Table VII. Substituent Effects in Tin Hydrides on TCNE Insertion[a]

stannane	M	TCNE, M	k_T, M^{-1} s^{-1} [b]
Me_3SnH	4.02×10^{-4}	3.0×10^{-5}	149 (2.17)
n-Bu_3SnH	2.28×10^{-4}	2.0×10^{-5}	612 (2.74)
i-Pr_3SnH	2.66×10^{-4}	2.0×10^{-5}	384 (2.58)
Ph_3SnH	6.40×10^{-4}	3×10^{-5}	2.87 (0.46)

[a] In acetonitrile at 25 °C. [b] Log k_T in parentheses.

Table VIII. Vertical Ionization Potentials of Trialkyl- and Tetraalkylstannanes

alkyl	R_3SnH[a] $I_D(1)$	R_3SnH[a] $I_D(2)$	R_4Sn, I_D
Me	9.96	10.60	9.69
Et	9.06	10.11	8.93
n-Bu	8.72	9.88	8.76
i-Pr	8.62	9.75	8.46

[a] $I_D(1)$ and $I_D(2)$ are associated with the R–M and R–H orbitals, respectively (see ref 20).

Other standard inhibitors such as oxygen, 2,6-di-*tert*-butylquinone, duroquinone, phenanthroquinone, chloranil, 2,6-di-*tert*-butyl-4-cresol, and phenothiazine also did not affect the rate of the insertion reaction.

Paramagnetic Intermediates in the Insertion Reaction. Two principal types of paramagnetic species can be detected during the insertion reaction. The TCNE radical, either as the anion radical or ion paired with the metal (i.e, $R_3MTCNE\cdot$), is ubiquitous in the reactions with R_3MH. It often dominates the ESR spectra of solutions since it is so persistent. On the other hand, the hydrogen atom H· is known to be quite transient, and immobilization in a frozen matrix was required to observe it, as described in the following section.

1. Tetracyanoethylene Radicals. The concentration of TCNE radicals which are built up during insertion varies with the metal and the solvent—generally in the order Sn > Ge > Si and CH_3CN > benzene > cyclohexane. However, integration of the overmodulated ESR signal indicates it to be a relatively minor byproduct in the thermal process. (The irradiation of the solution through a Pyrex filter leads to a large increase in its concentration.)

The line widths of the ESR spectra of TCNE anion radicals formed under these conditions are variable owing to modulations arising from spin exchange with unreacted TCNE (vide supra). The nitrogen hyperfine splittings are compared with

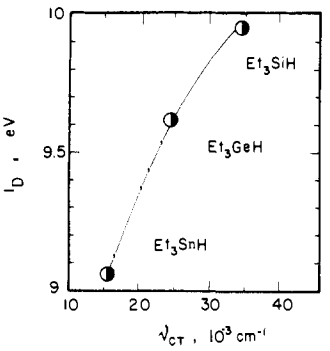

Figure 3. The relationship between the ionization potential (I_D) of metal hydrides and the energy ($h\nu_{CT}$) of the charge-transfer transition of the TCNE complex.

those of structurally analogous polycyanoalkyl radicals in Table IX. The latter are transient species produced by hydrogen abstraction from the corresponding diamagnetic precursor with photochemically generated *tert*-butoxy radicals[23] (eq 12).

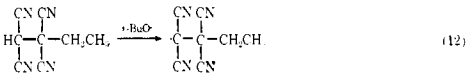

(12)

2. Chain Transfer with TCNE Radicals. Since TCNE radicals are generated in the presence of excess R_3MH during insertion, it is conceivable that hydrogen atom transfer may occur (eq 13). Indeed, such a chain-transfer process is germane

$$R_3MTCNE\cdot + R_3MH \longrightarrow R_3M(TCNE)H + R_3M\cdot \quad (13)$$

to the propagation sequence in the radical chain mechanism for insertion. The other step involving the addition of $R_3M\cdot$ to TCNE in eq 14 is expected to be rapid.

$$R_3M\cdot + TCNE \longrightarrow R_3MTCNE\cdot, \text{ etc.} \quad (14)$$

Although inhibition studies indicate that a free-radical chain mechanism is not operative (vide supra), it is important to rule out the involvement of TCNE radicals in *any* chain-transfer process with metal hydride. To test this possibility directly, *n*-$Bu_3SnTCNE\cdot$ was generated by the controlled potential electrolysis of *n*-$Bu_3Sn(TCNE)H$ in acetonitrile, and its spontaneous decay was monitored by following the decrease in the amplitude of the ESR signal. The second-order rate constant of 1.3×10^{-2} M^{-1} s^{-1} for the disappearance of *n*-$Bu_3SnTCNE\cdot$ in the presence of a tenfold excess of *n*-Bu_3SnH is more than 10^4 times slower than the rate constant k_T for insertion in Table III. Therefore, chain transfer in eq 13 cannot represent a viable step in the mechanism for hydrogen transfer to TCNE during the insertion process.

Charge-Transfer Complexes as Intermediates in Metal Hydride Insertion. Charge-transfer bands are observed in the absorption spectra of solutions containing metal hydride and TCNE. The use of relatively high concentrations of metal hydride (0.1–1 M) compared with that of TCNE (0.01 M) was necessitated by the rather low absorbance of these systems. It appears thus that the equilibrium constant in eq 15 is generally

$$R_3MH + TCNE \overset{K}{\rightleftharpoons} [R_3MH\ TCNE] \quad (15)$$

small. This conclusion is qualitatively supported by an analysis of the charge-transfer spectrum between Et_3GeH and TCNE by the Benesi–Hildebrand method.[24]

1. Spectral Studies. The charge-transfer bands are uniformly broad and weak, as is characteristic of intermolecular CT spectra derived from σ donors (R_3MH) and a π acceptor (TCNE).[25] The absorption maxima are highly dependent on the metal, the frequency ν_{CT} decreasing in the order Et_3SiH > Et_3GeH > Et_3SnH as listed in Table III. According to the valence bond description,[26] the frequency of the CT band

Table IX. ESR Parameters of α-Cyanoalkyl Radicals

cyanoalkyl radical	temp, °C	g	a_N, G
·TCNE[a]	−93	2.0030	5.5[d]
	25	2.0030	1.7[d]
·$C(CN)_2H$[b]	18	2.0023	2.75[e]
			19.25[f]
·$C(CN)_2C(CN)_2Et$[c]	18	2.0024	2.6[e]

[a] In acetonitrile solution from Et_3SiH, Et_3GeH, or Et_3SnH. [b] From malonitrile by photolysis of di-*tert*-butyl peroxide solution in benzene (transient). [c] From 1,1,2,2-tetracyanobutane as in footnote *b* (transient). [d] Nonet. [e] Quintet. [f] Doublet due to proton splitting.

corresponds, in the simplest form, to the energy ($h\nu_{CT}$) required to transfer an electron from the donor to the acceptor, i.e., eq 16. For weakly associating systems such as the σ–π

$$[R_3MH\ TCNE] \xrightarrow{h\nu_{CT}} [R_3MH^+\cdot\ TCNE^-\cdot] \quad (16)$$

complexes involved here, the energy of the absorption maximum is approximated by[27] eq 17, where I_D and E_A refer to the

$$h\nu_{CT} = I_D - E_A - (G_1 - G_0) \quad (17)$$

vertical ionization potential of the donor and the electron affinity of the acceptor, respectively. G_0 is the energy of the "no bond" interaction and G_1, the dominant term, involves the coulombic interaction of $R_3MH^+\cdot$ and $TCNE^-\cdot$ in the excited ion-pair state. For a series of CT complexes with a common acceptor (TCNE), ν_{CT} should parallel I_D as shown in Figure 3 for the various group 4a metal hydrides. The trend is unmistakable, but the deviation from linearity suggests that the intermolecular terms G_0 and G_1 are not wholly constant with this series of donors.

2. Persistence of the Charge-Transfer Band. Although the charge-transfer band appears instantly upon the addition of metal hydride to the TCNE solution, it does not persist. The rate of disappearance correlates strongly with the energy ($h\nu_{CT}$) of the charge-transfer transition. Thus, the CT complex of Et_3SnH and TCNE is observed only as a fleeting blue color. However, the extremely transient absorption spectrum of this complex could be obtained by a point by point determination of the absorbance using a Durrum-Gibson stopped flow spectrophotometer. The disappearance of the CT band (followed under pseudo-first-order conditions) proceeded with a rate constant, $k = 6.9 \times 10^2$ M^{-1} s^{-1} at 25 °C in acetonitrile. This value compares favorably with the second-order rate constant determined for insertion in Table III.

The CT band from Et_3GeH and TCNE persists for ~5 min and is only observable in the presence of acetic acid to neutralize the TCNE anion radical. Qualitatively it disappears at a rate comparable with that of TCNE insertion.

The maximum of the CT band Et_3SiH and TCNE occurs further into the ultraviolet, and it could be resolved from the tail of the π–π^* transition of TCNE only as a difference spectrum. The CT band also disappears slowly at a rate comparable to the slow rate of insertion of Et_3SiH and TCNE.

3. Photochemistry of the Charge-Transfer Complex. Irradiation of the charge transfer complex was carried out both in solution at low temperatures to obviate the thermal process and in a frozen matrix to observe the intermediates.

a. Photoinduced insertion of the metal hydride was examined by direct irradiation of the charge-transfer band of the complex. The CT band of R_3SnH–TCNE absorbs conveniently at the blue end of the spectrum, but the thermal reaction occurs much too rapidly to slow down at low temperatures sufficient to unequivocally demonstrate the photoinduced insertion. Thermal insertions of the germanium analogs also occur rapidly. However, by carrying out the photolysis at −40 °C under

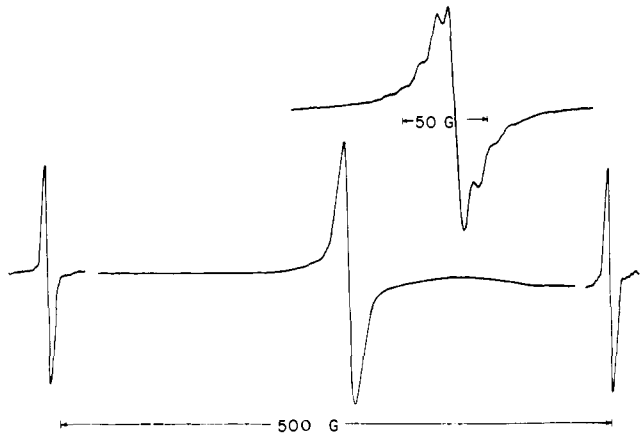

Figure 4. ESR spectrum obtained by the direct irradiation of the charge-transfer complex [*n*-Bu_3GeH-TCNE] in 1:1 v/v acetonitrile-1,2-dichloropropane through a Pyrex filter at −175 °C, showing hydrogen atoms (×25) and TCNE anion radical. Inset at higher resolution (×5) shows nitrogen hyperfine splittings of central line.

very dilute conditions with parallel control experiments, it could be shown (see Experimental Section) that insertion is induced photochemically. (Although the rate of silane insertion is convenient for these studies, the charge-transfer band at 290 nm is too close to the π-π^* transition of TCNE.)

b. Paramagnetic intermediates are observed if the irradiation of the charge-transfer complex is carried out directly in the cavity of the ESR spectrometer. Since these intermediates are quite transient, the photoinduced reactions were performed in a frozen matrix at −175 °C. The ESR spectrum obtained under these conditions consists of a mixture of hydrogen atoms and TCNE radicals which are shown in Figure 4. The doublet with a hyperfine splitting of 505 G is clearly due to H·,[28] and the inset shows the resolution of the central line due to TCNE radical (into the nitrogen hyperfine splittings of a_N = 5.5 G, g = 2.0030), anisotropically broadened.[29] Under constant irradiation at −175 °C, these paramagnetic species build up at the same rate. When the light is extinguished, both radicals disappear rapidly. Control experiments showed that no paramagnetic species are produced unless *both* components are present.

Mass Spectral Cracking Patterns of Metal Hydrides. The examination of the mass spectra of trialkylmetal hydrides was undertaken in order to obtain information on the relative bond dissociation processes involving alkyl-metal and hydrido-metal scission from the parent molecular ion, i.e., eq 18 and 19. In-

$$R_3MH^+ \longrightarrow R_2MH^+ + R\cdot \quad (18)$$

$$R_3MH^+ \longrightarrow R_3M^+ + H\cdot \quad (19)$$

deed, the three ions in eq 18 and 19 are the principal species formed from Et_3SiH, Et_3GeH, and Et_3SnH.[30] The relative amounts of R_3MH^+, R_2MH^+, and R_3M^+ are more or less insensitive to ionizing voltages of 20, 40 and 70 V (nominal) as shown in Figure 5. If we assume that R_2MH^+ and R_3M^+ are only derived from the fragmentation of the parent molecular ion,[30b] then the ratio, R_2MH^+/R_3M^+, is a direct measure of the competition in eq 18 and 19. From an examination of Figure 5, we conclude that alkyl-metal fragmentation is preferred over hydrido-metal fragmentation in eq 19 by at least a factor of 10.

Reduction of Quinones with Metal Hydrides. Quinones are reduced spontaneously by trialkyl metal hydrides ultimately to hydroquinones.[31] For example, Et_3SiH reacts with 2,3-dichloro-5,6-dicyanoquinone (DDQ) in acetonitrile at room temperature to afford the corresponding hydroquinone. The presence of the semiquinone radical ($DDQ^-\cdot$ is also indicated

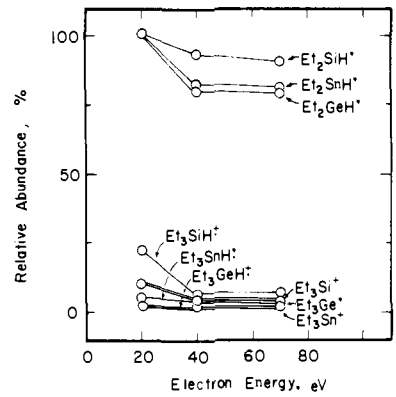

Figure 5. Mass spectral cracking pattern of Et_3SnH, Et_3GeH, and Et_3SiH at various ionizing energies (nominal).

Table X. Standard Reduction Potentials of TCNE and Quinones in Acetonitrile at 25 °C

acceptor	$E°$, V[a]	$i_p(c)/i_p(a)$[b]	Δ,[c] mV
tetracyanoethylene	+0.222	1.01	55
2,3-dichloro-5,6-dicyanoquinone	+0.510	1.02	56
tetrachloro-*p*-benzoquinone	+0.011	1.00	58
chloro-*p*-benzoquinone	−0.350	1.02	60
p-benzoquinone	−0.507	1.02	68

[a] Relative to saturated NaCl-SCE reference with platinum electrode and Et_4NBr as supporting electrolyte. [b] Peak current ratio of the cathodic and anodic waves. [c] Voltage separation of cathodic and anodic peaks at sweep rates of 100 mV s^{-1}.

by its ESR spectrum (g = 2.0038). Reactions of quinones with metal hydrides are thus similar to the reaction with TCNE. Hydrogen transfer can be formulated as the first step in the reduction (eq 20).

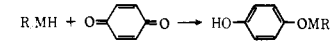

(20)

In order to extend our studies with TCNE, we also examined the rates of reaction between metal hydrides and quinones with various reduction potentials. The standard reduction potentials of TCNE and those quinones in Table X were redetermined in acetonitrile by cyclic voltammetry. To ensure for reversibility, the peak-current ratio for the cathodic and anodic waves $i_p(c)/i_p(a)$ was determined as 1, and the voltage separation was shown to be close to the theoretical value of 59 mV.

The second-order rate constants in acetonitrile are listed in Table XI for 1,4-benzoquinone (BQ), chloroquinone (CQ), chloranil (CA), and 2,3-dichloro-5,6-dicyanoquinone (DDQ) with four stannanes, Me_3SnH, *n*-Bu_3SnH, *i*-Pr_3SnH, and Ph_3SnH. The rates of reduction of BQ and CQ which are relatively slow were readily followed by monitoring the decrease in the Sn-H absorption in the IR spectra. The kinetics of the others were determined spectrophotometrically by utilizing the electronic absorptions for TCNE (270 nm, ϵ 15 500), CA (368 nm, ϵ 278), and DDQ (500 nm, ϵ 109). The rates of reduction of DDQ were determined by stopped-flow techniques. The rates of reaction of *n*-$BuSn_3SnD$ were measured in the same way and used in the determination of the deuterium kinetic isotope effect.

Discussion

The mechanistic study of TCNE insertion into metal hydrides is of general interest for two principal reasons. First, little is known about how hydrogen is transferred during re-

Table XI. Reduction of Quinones by Trialkyltin Hydrides[a]

quinone compd	quinone M	R_3SnH R	R_3SnH M	rate constant,[b] $M^{-1}\ s^{-1}$
2,3-dichloro-5,6-dicyanoquinone	6.60×10^{-4}	*n*-Bu	1.42×10^{-2}	676 (2.83)
	6.60×10^{-4}	Me	1.72×10^{-2}	125 (2.10)
	6.60×10^{-4}	*i*-Pr	1.32×10^{-2}	105 (2.02)
	2.40×10^{-3}	Ph	1.42×10^{-2}	1.62 (0.21)
tetrachloro-*p*-quinone	3.30×10^{-4}	*n*-Bu	2.28×10^{-2}	0.36 (−0.45)
	3.20×10^{-4}	Me	3.65×10^{-2}	0.187 (−0.73)
	3.20×10^{-4}	*i*-Pr	2.66×10^{-2}	0.137 (−0.86)
	3.10×10^{-4}	Ph	1.13×10^{-1}	7.6×10^{-4} (−3.12)
chloro-*p*-benzoquinone	1.02	*n*-Bu	4.14×10^{-2}	2.2×10^{-2} (−1.65)
	0.257	Me	3.35×10^{-2}	2.4×10^{-3} (−2.62)
p-benzoquinone	1.16	*n*-Bu	2.53×10^{-2}	2.9×10^{-4} (−3.53)
	1.25	Me	4.20×10^{-2}	1.6×10^{-4} (−3.79)

[a] In acetonitrile at 25 °C. [b] Logarithms in parentheses.

Scheme I. Radical Chain

$$R_3Sn\cdot + TCNE \longrightarrow R_3SnTCNE\cdot \quad (21)$$

$$R_3SnTCNE\cdot + R_3SnH \longrightarrow R_3Sn(TCNE)H + R_3Sn\cdot, \text{ etc.} \quad (22)$$

Scheme II. Hydrogen Transfer

$$R_3SnH + TCNE \xrightarrow{k} R_3Sn\cdot + HTCNE\cdot \quad (23)$$

$$R_3Sn\cdot + HTCNE\cdot \xrightarrow{fast} R_3Sn(TCNE)H \quad (24)$$

Scheme III. Charge Transfer

$$R_3SnH + TCNE \overset{K_c}{\rightleftharpoons} [R_3SnH\,TCNE] \xrightarrow{k_T} [R_3SnH^+\cdot TCNE^-\cdot] \quad (25)$$

$$[R_3SnH^+\cdot TCNE^-\cdot] \xrightarrow{fast} R_3Sn(TCNE)H \quad (26)$$

ductions with metal hydrides. Second, the hydrogen transfer from metal hydrides bears formal resemblance to the mechanism of similar processes with dihydropyridine and related compounds as hydride donors in biological oxidation–reduction processes, for which there is considerable recent interest.[32-35]

In this discussion we shall first describe how the charge-transfer interaction plays an important role in the mechanism of hydrogen transfer from metal hydrides in TCNE insertion. Focussing on kinetic isotope effects, we then will delineate these processes from hydride transfers in the context of dihydropyridine systems.

I. Mechanism of Hydrogen Transfer from Metal Hydrides in TCNE Insertion. The addition of metal hydrides, particularly of the group 4a elements to unsaturated functional groups most commonly proceeds via a homolytic chain mechanism.[36] The well-established sequence of propagation steps is summarized in Scheme I, as it may pertain to a tetracyanoethylene addend. Such a radical-chain mechanism, however, cannot apply to TCNE insertion for two compelling reasons. First, the adduct radical, $R_3SnTCNE\cdot$, which we can generate independently, does not react with R_3SnH in eq 22 at rates sufficient to account for the insertion process. Furthermore, the absence of a deuterium kinetic isotope effect for insertion indicates that hydrogen transfer is not rate limiting as suggested by Scheme I, since the addition in eq 21 must be rapid. Secondly, extensive tests with inhibitors show that TCNE insertion does not proceed via a radical-*chain* process. That is not to say, however, that paramagnetic species are not intermediates.

Indeed, free radicals can be detected during the insertion reaction; viz., the TCNE radical as a relatively stable species in Table IX. Such species may be derived by a mechanism involving direct hydrogen transfer in the second-order activation process in eq 23. However, Scheme II can be eliminated on the basis of the deuterium kinetic isotope effect and the relative reactivities of alkyl- and arylstannanes. Thus, k_H/k_D for hydrogen transfer from *n*-Bu_3SnH to either cyclohexyl or *tert*-butyl radical is ~2.[37] Carlson and Ingold also found Ph_3SnH to be more reactive than *n*-Bu_3SnH—both with regard to the rate of hydrogen atom transfer as well as the reactivity of the stannyl radical. By contrast, the TCNE insertion shows no kinetic isotope effect (Tables V and VI), and Ph_3SnH is at least 200 times *less* reactive than *n*-Bu_3SnH (Table VII).

An alternative mechanism for insertion proceeding via paramagnetic intermediates is represented by a charge-transfer interaction followed by electron transfer (Scheme III). Indeed, the electron-transfer mechanism in Scheme III receives support from the observation of charge-transfer bands due to R_3MH–TCNE, which disappear at the same rates as the insertion reactions proceed (Table III).[38]

A. Thermal Activation of Electron Transfer. According to Scheme III, the activation energy E_T for electron transfer in the rate-limiting eq 25 should be related to the energetics of electron detachment from the donor R_3MH as well as that of electron attachment to the acceptor TCNE. The first-order relationship for the enthalpy change is shown in eq 27[13] where

$$\Delta H_T = I_D - E_A - e^2/\bar{r}_{D^+A^-} \quad (27)$$

I_D and E_A are the ionization potential of the R_3MH donor and electron affinity of the TCNE acceptor, respectively. Indeed, the strong dependence of the insertion rate on the metal, i.e., Sn ≫ Ge ≫ Si, readily accords with the large differences in the ionization potentials of these metal hydrides in Figure 3.

The last term in eq 27 represents the contribution from the electrostatic potential in the ion pair with mean separation of $\bar{r}_{D^+A^-}$ as illustrated in Figure 6. Assuming that ΔH_T parallels the activation energy,[39] the comparison of the rate data (i.e., log k_{R_3SnH}) in Table VII does show a general correlation with the ionization potentials I_D of a limited number of stannanes in Table VIII. Using the same data an alternative, and perhaps more relevant, comparison also evolves from an examination of the reactivities of various stannanes with reference to a standard such as n_3-Bu_3SnH (which is designated as k_0). It is noteworthy that the logarithm of these relative reactivities correlates linearly with the Taft inductive parameter[40] σ^* expressed in the form of the linear free-energy relationship shown in eq 28. The sensitivity to polar effects is given by the

$$\log (k_{R_3SnH}/k_0) = -3\sigma^* = \rho^*\sigma^* \quad (28)$$

slope $\rho^* = -3$, which reflects a substantial development of positive charge in the transition state for insertion, as expected for an electron-transfer process. Since it has already been shown[41] that HOMO energies of various alkyltin compounds can be related to the σ^* values of the alkyl ligands, ρ^* in eq 28 is a measure of the sensitivity of the R_3MH moiety to ionization in the transition state shown in (29) for the TCNE insertion process.

$$[R_3MH\,TCNE \longleftrightarrow R_3MH^+\cdot TCNE^-\cdot]^* \quad (29)$$

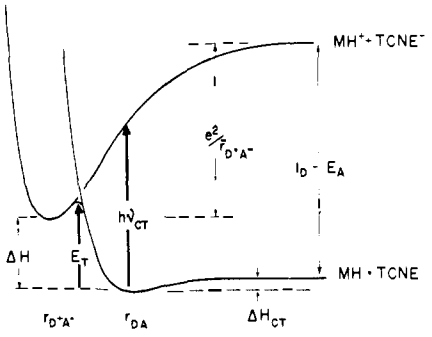

Figure 6. The relationship between thermal (E_T) and photochemical activation ($h\nu_{CT}$) of electron transfer proceeding from the charge-transfer complexes derived from metal hydride donors to TCNE acceptor.

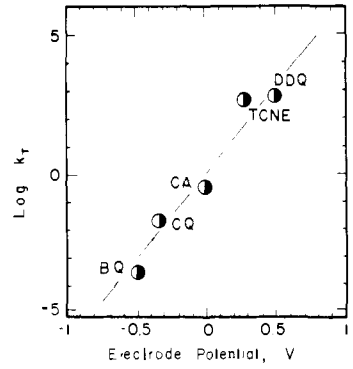

Figure 7. Correlation of the rates of n-Bu_3SnH reduction with the reduction potentials ($E°$) of various acceptors in acetonitrile at 25 °C.

A high degree of charge transfer in the transition state for hydrogen transfer from metal hydrides is also indicated by the strong dependence on the reduction potential of the acceptor. Thus, Figure 7 illustrates the rates of stannane reaction with a series of electron acceptors of varying reduction potentials in which the linear correlation of rates extends to seven orders of magnitude, i.e., eq 30 where $E°$ is the reversible reduction

$$\log k_{R_3SnH} = 6.2E° + \text{constant} \qquad (30)$$

potential of various acceptors in Table X, including TCNE and various quinones. It is noteworthy that the slope of 6.2 is approaching the theoretical limit of 8.5 predicted by Marcus theory[42,43] for a complete outer-sphere process for electron transfer.

Charge development in the transition state for TCNE insertion thus derives from the strong correlations of the rates (log k) with the energetics of both electron detachment and electron attachment from the R_3MH donor and the acceptor, respectively. The high sensitivity to the polarity of the solvent in Table IV also accords with a strongly polar transition state.

B. Photochemical Activation of Electron Transfer. The most direct and compelling evidence for the charge transfer mechanism of TCNE insertion in Scheme III is obtained from the clear-cut demonstration that the activation process in eq 25 is photochemically pumped at low temperatures under conditions in which the thermal reaction is too slow. According to the well-established Mulliken theory[26,27] the charge-transfer band for weak σ–π complexes of the type described here is largely associated with the optical transition to produce an excited ion pair (eq 31 as a result of electron transfer from the

$$[R_3MH\,TCNE] \xrightarrow{h\nu_{CT}} [R_3MH^+\cdot TCNE^-] \qquad (31)$$

R_3MH donor to the TCNE acceptor. Therefore, direct irradiation of the charge-transfer band would effectively lead to population of the ion-pair states. It follows that the photoinduced insertion reaction which is observable at low temperatures where the thermal process is negligible, must also proceed via these or similar ion pairs. The interrelationship between ion pairs formed thermally (E_T) and photochemically ($h\nu_{CT}$) is illustrated in Figure 6.[44]

C. Paramagnetic Intermediates. Direct Observation. Importantly, photochemical pumping of the charge-transfer band also allows the direct detection of metastable intermediates in the fast followup reactions represented in eq 26, subsequent to rate-limiting electron transfer. Thus, irradiation of a mixture of R_3GeH and TCNE in a frozen matrix leads to hydrogen atom and TCNE anion radical, both detectable by their characteristic ESR spectra. Such intermediates must derive from fragmentation within the ion pair, e.g., eq 32. Under

$$[R_3GeH^+\cdot TCNE^-] \xrightarrow{fast} [H{\cdot}\,R_3Ge^+\,TCNE^-] \qquad (32)$$

constant irradiation, both radicals build up coincidentally and attain a quasi steady state concentration shown in Figure 8. The latter is a result of competition from the rapid cage collapse to produce the insertion adduct in eq 33, which can be

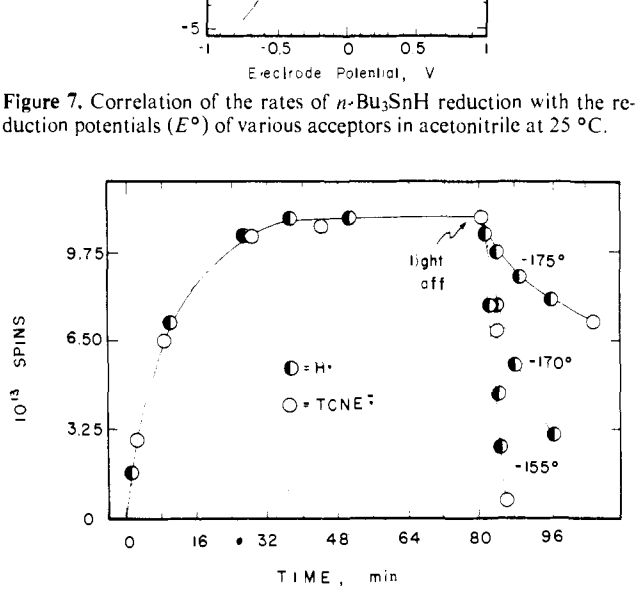

Figure 8. Production of hydrogen atom, ◐, and TCNE anion radical, ○, during the constant irradiation of the charge-transfer complex [n-Bu_3GeH-TCNE] at −175 °C. Decay of the ESR signal following light turnoff is shown at several temperatures.

$$[H{\cdot}\,R_3Ge^+\,TCNE^-] \xrightarrow[\text{collapse}]{} R_3GeTCNEH \qquad (33)$$
$$\xrightarrow[\text{diffuse}]{} H\cdot + R_3GeTCNE, \text{ etc.} \qquad (34)$$

readily demonstrated by shuttering the light and then following the radical decays (right side of Figure 8). The rapidity of this process even in a frozen matrix is doubtlessly due to the high mobility of hydrogen atoms.[45,46] (In these experiments, it is noteworthy that the ESR spectrum of the alkyl radical derived by alkyl-metal cleavage is absent.)

According to this formulation, TCNE radicals are initially formed as cage intermediates from a rate-limiting electron transfer. The ubiquity of TCNE radicals as products arises from a side reaction resulting from the diffusion of hydrogen atoms out of the cage, as in eq 34. The absence of an observable CIDNP in the NMR spectra of the products (see Experimental Section) may be related to the rapidity of these cage processes.[47]

The facility of the dark reactions leading to the insertion adducts subsequent to the rate-limiting electron transfer depends to a large extent on the metastability of the metal hydride moiety, $R_3MH^+\cdot$ in the ion pair in eq 32. The ready fragmentation of such a cation radical is supported (1) by the irreversibility of the cyclic voltammogram of R_3MH and (2) by analogy to the behavior of the peralkyl analogues $R_4M^+\cdot$ studied earlier.[13] However, there are two important anomalies with this formulation which must be resolved. First, the selectivity in the fragmentation of $R_3MH^+\cdot$ derived from the mass spectral cracking of R_3MH does not accord with the selectivity in TCNE insertion.[48] Secondly, photoelectron spec-

Table XII. Comparison of Trialkylmetal Hydrides and Tetraalkylmetals as Electron Donors

organometal	I_D, eV	ν_{CT},[a] eV	log k_T,[b] M^{-1} s^{-1}
n-Bu_3SnH	8.72	1.9	+2.79
n-Bu_4Sn	8.76	3.02	−2.04
Et_3GeH	9.62	3.02	−1.77
Et_4Ge	9.41	3.72	−3.80
Et_3SiH	9.95	4.28	−4.49
Et_4Si	9.78		[c]

[a] Frequency of the charge-transfer band with TCNE in chloroform. [b] In acetonitrile at 25 °C. [c] Too slow to measure.

troscopy in Table VIII shows that the HOMO in R_3MH is the alkyl-metal rather than the hydrido-metal σ-bonding orbital, and thus insertion in R_3MH apparently does not proceed via the frontier orbital. The resolution of this conundrum may lie in the inherent differences between highly energetic radical cations of R_3MH generated by electron impact in the gas phase and those generated in ion pairs during charge transfer in solution. Indeed, the latter does raise the question as to the intimate nature of the ion pair $R_3MH^+ \cdot TCNE^{-}\cdot$ as a reactive intermediate in insertion. An issue of particular relevance is how close the ions lie together, since the $TCNE^{-}\cdot$ moiety could affect the behavior of $R_3MH^+\cdot$ in the ion pair. In order to discuss this point, we wish to compare metal-hydride insertion to metal-alkyl insertion in which steric effects have already been assessed.[13]

D. Ion Pairs in Metal-Hydride and Metal-Alkyl Insertions. Metal-alkyl insertion of TCNE occurs readily with a series of peralkyl derivatives of Si, Ge, and Sn differing in steric requirements for process 35.[9] The metal-alkyl insertion in eq 35

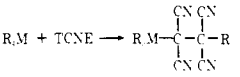

(35)

is therefore completely analogous to metal-hydride insertion in eq 1. Furthermore, the same basic charge transfer mechanism in Scheme IV has been demonstrated for metal-alkyl insertion[13] (eq 36 and 37). Thus, metal-hydride insertion with R_3MH in Scheme III and metal-alkyl insertion with R_4M in Scheme IV have two important features in common: (1) the formation of charge-transfer complexes with TCNE and (2) a thermal activation process E_T for electron transfer. We deduce from both that the interaction of R_3MH with TCNE is more intimate than that of R_4M. Thus, the frequency of the charge-transfer band of R_3MH–TCNE always occurs at significantly lower energy than that of R_4M–TCNE as shown in Table XII. According to eq 17, the difference is readily attributed to an increased electrostatic potential G_1 as a result of the closer approach of R_3MH than R_4M to TCNE in the CT complex. The same conclusion derives from eq 27 viewed as faster rates of TCNE insertion in R_3MH compared with those of R_4M with the same ionization potential, as also summarized in Table XII.

The detailed study of steric effects of R_4Sn insertion showed that electron transfer in Scheme IV (eq 36b) is an inner-sphere process.[13] Since ν_{CT} and E_T are both highly sensitive to the intermolecular separation of R_4M and TCNE (as mediated by the steric bulk of alkyl ligands),[22] we conclude that the charge- (electron-) transfer interaction is dominated by the small size of the hydrogen ligand, which allows a more intimate approach of TCNE to the metal center of R_3MH than of R_4M. Basically the same reasoning applies to an intramolecular competition in which the preference for hydrogen over alkyl

Scheme IV

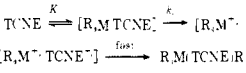

(36)

(37)

Scheme V. Hydride Transfer

(38)

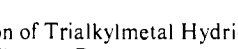

(39)

insertion in R_3MH results from the preferential interaction of TCNE with HOMO-1 centered on the H–M bond rather than the frontier orbital (HOMO), as a result primarily of an increase in electrostatic energy sufficient to overcome the discrepancy in the orbital energies.[49] Such a tight transition state is to be distinguished from one involving direct hydride transfer to be discussed in the next section, since ESR studies show that paramagnetic species are actual intermediates.

II. Electron-Transfer and Hydride-Transfer Mechanisms. A Comparison of Kinetic Isotope Effects. The electron-transfer mechanism for hydrogen transfer from metal hydrides in Scheme III has its counterpart in a direct hydride transfer, e.g., Scheme V. The difference between reactions proceeding by hydride transfer and electron transfer is subtle since the activation process in both cases requires considerable electron release from the donor. However, they are mechanistically distinct—the hydrogen is directly transferred during the rate-limiting step in the hydride mechanism, whereas the electron-transfer mechanism is a two-step process in which the hydrogen is transferred subsequent to rate-limiting electron transfer. The problem of distinguishing between these mechanisms is a general one, a most relevant example applying to dihydropyridines and related compounds as "hydride" donors in biological oxidation-reduction processes.[32-35] Indeed, we are capitalizing on the similarity between metal hydrides and dihydroaromatics as hydrogen donors to make direct comparisons between the two systems, using the recent study of Colter and co-workers[50] on the oxidation of N-methylacridan by various acceptors as an example.

The deuterium kinetic isotope effect provides potentially the most direct method of distinguishing between the mechanisms in Schemes III and V. However, the use of kinetic isotope effects is not without some ambiguities, since it is known that the magnitude of k_H/k_D is sensitive to the driving force (ΔH) as well as steric, polar and element effects.[51-53] The isotope effect is generally maximum when ΔH is close to 0, and hydrogen transfer is nearly symmetrical in the transition state. Lewis and Ogino[54] have suggested that the falloff in k_H/k_D as a result of the symmetry effect[55] is important with elements beyond the first row such as silicon, germanium, and tin. Thus, it is possible for the small isotope effects in Tables V and VI to represent hydride transfers from metal hydrides to TCNE which proceed via very early (or late) transition states.

Figure 9 shows, however, that k_H/k_D for n-Bu_3SnH is *invariant* with various acceptors of differing reduction potentials and sufficient to span a range of 10^7 in rates of insertion. In marked contrast, hydride transfer from N-methylacridan to the same or similar series of acceptors shows a highly variable deuterium kinetic isotope effect. The strong dependence of k_H/k_D on the reduction potential $E°$ of the acceptor is consistent with a transition state for hydride transfer from N-methylacridan, whose location along the reaction coordinate varies strongly with the strength of the acceptor, i.e., the driving force. In contrast, electron transfer from the metal hydride shows no such variation.

The effect of solvent on k_H/k_D provides a second measure for comparing the displacement of the transition states in hydride transfers and in electron transfers. Thus the activation energies, correlated as rates (log k), should parallel the progress of the transition state along the reaction coordinate if hydrogen is directly transferred to a common series of acceptors. Indeed, hydride transfer from N-methylacridan in solvents of various polarity results in a large change in k_H/k_D as well as in the second-order rate constant as shown in Figure 10. In the reactions of n-Bu_3SnH, the second-order rate con-

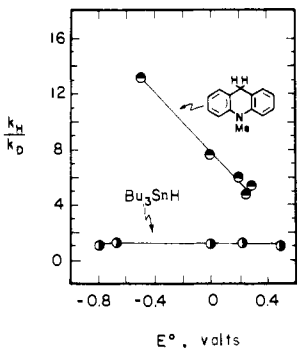

Figure 9. Comparison of deuterium kinetic isotope effects in ● hydride transfer from *N*-methylacridan (from Colter et al.[50]) with ◑ electron transfer from *n*-Bu_3SnH as a function of the reduction potential ($E°$) of the donor.

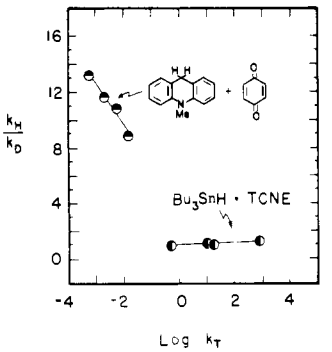

Figure 10. The effect of solvent polarity on the kinetic isotope effect shown in ● hydride transfer from *N*-methylacridan to quinone (from Colter et al.[50]) and in ◐ electron transfer from *n*-Bu_3SnH to TCNE.

stants also experience large changes, increasing by a factor of 10^3 from cyclohexane to acetonitrile. However, there is no significant trend in k_H/k_D.

The absence of a trend in the kinetic isotope effect with changes in either the strength of the acceptor or the solvent polarity, despite drastic changes in the observed rate constants, represents strong evidence for ruling out hydride transfer in Scheme V in the insertion of metal hydrides into TCNE. Thus, these studies of the kinetic isotope effects support the chemical, photochemical and esr studies in the foregoing section, and together they provide compelling evidence for the electron-transfer mechanism in Scheme III for metal hydride insertion.

In the electron-transfer mechanism in Scheme III, transfer of hydrogen occurs subsequent to rate-limiting electron transfer. Accordingly, the deuterium kinetic isotope effect, if such is manifested, is a secondary effect and related only to the electron-transfer step. Under these circumstances, the isotope effect is expected to be nil or small, since it is related only to the small difference in HOMO energies of the α-protio and α-deuterio metal hydrides.[56] In a related context, Pryor and Hendrickson[57] have found isotope effects in the range between 1.1 and 1.5 to be appropriate for distinguishing electron transfer from S_N2 mechanisms in displacements with various β-deuterated nucleophiles.

Conclusion

The development of charge- (electron-) transfer as a general mechanism for hydride transfer provides a basis for the spontaneous initiation of a variety of radical-chain processes previously observed with metal hydrides.[3,7,36] The electron donor properties of metal hydrides coupled with the strength of the acceptor provide relevant guidelines for the delineation of these mechanisms. Moreover, the importance of solvation in charge-transfer processes[18] cannot be overemphasized, and changes in solvent polarity may be sufficient to alter the course of hydrogen transfer reactions. More importantly, charge-transfer interactions make significant contributions to metal hydride reactivity in general, even in those reactions proceeding via concerted mechanisms involving hydride transfer, as shown by a comparison of our results with hydride transfer from dihydropyridine derivatives to various acceptors.[50]

Experimental Section

Materials. The trialkyltin hydrides R_3MH were prepared from the corresponding trialkyltin chlorides by reduction with lithium aluminum hydride or deuteride.[58,59] The trialkyltin chlorides were obtained by disproportionation of the tetraalkyltin with $\frac{1}{3}$ mol of stannic chloride, by heating to reflux followed by vacuum distillation.[58] The tetraalkyltin compounds were prepared from stannic chloride and the appropriate Grignard reagent using a standard procedure: Et_3SnH, bp 70 °C (50 mm);[58] *n*-Bu_3SnH, bp 86 °C (1 mm);[58] Me_3SnH, bp 60 °C (752 mm);[58] *i*-Pr_3SnH, bp 84 °C (15 mm);[58] and Ph_3SnH, bp 170 °C (1 mm).[58] The germanium analogues were prepared by a similar procedure: Et_3GeH, bp 125 °C (752 mm)[59] and *n*-Bu_3GeH, bp 124 °C (20 mm).[59] Triethylsilane, by 110 °C (752 mm)[60] was also prepared by this procedure.

Tetracyanoethylene was obtained as a generous sample from Du Pont and triply resublimed in vacuo. Reagent grade acetonitrile was refluxed over calcium hydride, treated with potassium permanganate, and redistilled from phosphorus pentoxide through a 19-plate bubble plate column.[13] Reagent grade diethyl ether was redistilled from sodium benzophenone ketyl in vacuo. Spectrograde cyclohexane and methylene chloride were degassed but otherwise used without further purification.

Handling and Storage of Metal Hydrides. Metal hydrides, particularly trialkyltin hydrides, are susceptible to decomposition by heat, silicone grease, and metallic surfaces.[61] Reproducible results are difficult to obtain unless extreme caution is exercised in their handling and storage. Glassware cleaned with chromic acid cleaning solution must be avoided, but those washed with a solution of potassium hydroxide in ethanol, followed by numerous and thorough rinsings with water, gave reproducible results. The stannanes were transfered with an all-glass hypodermic syringe and stored at −20 °C under an argon atmosphere in Schlenk flasks equipped with Teflon stopcocks. All hydrides were redistilled in vacuo immediately prior to use.

Trialkylstannane Adduct to TCNE. Isolation and Characterization. In a typical procedure, a solution of 0.34 g (2.66 mmol) of TCNE in 20 mL of toluene was cooled to −10 °C and 2.65 mmol of Et_3SnH added. After the mixture was stirred for 15 min, the pale yellow solid was removed by filtration, washed with three portions of deaerated toluene, and dried in vacuo: yield, 0.67 g (76%). Alternatively, a slurry of 0.12 g (0.94 mmol) of TCNE in 5 mL of cyclohexane was treated with 0.24 mL (0.95 mmol) of Et_3SnH. The mixture was stirred for 6 h during which the TCNE slowly dissolved and reacted to produce a yellow powder. Filtration, followed by several toluene washes, afforded $Et_3Sn(TCNE)H$, which was reprecipitated several times from acetonitrile–toluene mixtures. Anal. Calcd for $C_{12}H_{16}N_4Sn$: C, 43.15; H, 4.53; N, 16.78; Sn, 35.54. Found: C, 43.31; H, 4.70; N, 16.95; Sn, 35.31. Numerous and varied attempts were made to grow crystals of the various stannane adducts, but they were all uniformly unsuccessful. Despite their physical appearance and absence of any paramagnetic impurities, the absence of X-ray diffraction patterns proved the colorless solids to be amorphous.

The insertion reaction in acetonitrile afforded several products. First, the pale yellow precipitate was contaminated with the radical $Et_3SnTCNE\cdot$, which could not be separated by reprecipitation. In addition, H_2TCNE, which is soluble in acetonitrile, was isolated in 9% yield after solvent removal, followed by sublimation of the residual solid in vacuo: NMR δ 4.93 (1 H, s). Small amounts of adventitious water in acetonitrile caused large changes in the NMR spectrum (δ 3.37 (1 H, s), 1.47 (15 H, m)) of the insertion adduct. In solutions made up from acetonitrile which was not especially dried, the unique proton appeared as a broad resonance at δ 2.4–3.2, which is intermediate between that at 3.37 and the water resonance at δ 2.10. The proton exchange in the adduct is described below.

Trialkylsilane Adducts to TCNE. Hydrolysis. The addition of Et_3SiH to TCNE in acetonitrile affords H_2TCNE and hexamethyldisiloxane as the only identifiable products. Thus, H_2TCNE was

isolated in 90% yields by solvent removal in vacuo, followed by sublimation of the residue. Examination of the IR spectrum of the solvent removed in this manner showed a strong absorption at 1100 cm^{-1} which was identical with that of an authentic sample of hexamethyldisiloxane. Similarly, gas chromatography of this solution on a 15-ft SE-30 silicone column at 250 °C showed hexamethyldisiloxane (but no hexamethyldisilane) in amounts corresponding to 95% (internal standard method), according to the stoichiometry, $Et_3Si(TCNE)H + H_2O \rightarrow Et_3SiOH + H_2TCNE$ followed by the condensation reaction, $2Et_3SiOH \rightarrow (Et_3Si)_2O + H_2O$.[59]

In order to remove water completely from the system, acetonitrile and Et_3SiH were both separately made up as pastes with large excesses of powdered calcium hydride. After sitting for 2 h, both mixtures were vacuum transferred to a quartz tube (previously dried at 200 °C for 24 h) containing TCNE. Reaction in the sealed tube afforded no H_2TCNE. Only the red material was detected by its characteristic NMR spectrum (δ 7.8 (s)), as described later.

The kinetics of Et_3SiH insertion was unchanged under these various conditions. Thus, the second-order rate constant k for the formation H_2TCNE followed by its NMR spectrum at δ 5 ppm in anhydrous, but unprepared, acetonitrile (containing 8×10^{-3} M water) was $2.9 \pm 0.4 \times 10^{-5}$ M^{-1} s^{-1}. The same rate was obtained ($k = 3.3 \pm 0.2 \times 10^{-5}$ M^{-1} s^{-1}) by following TCNE disappearance by its absorbance at 270 nm (ϵ 1.55×10^4 cm^{-1}). Finally, under rigorously anhydrous conditions, the rate of insertion followed by the disappearance of the IR band of Et_3SiH at 2000 cm^{-1} was $3.1 \pm 0.2 \times 10^{-5}$.

Trialkylgermane Adducts to TCNE. Triethylgermane (0.21 mmol) and TCNE (0.20 mmol) in 0.5 mL of CD_3CN were contained in an NMR tube with 0.50 mmol of H_2O and 0.16 mmol of CH_2Cl_2 as an internal standard. After 10 min, only H_2TCNE (90%) and triethylgermanol or the oxide (90%) was detected by an examination of the NMR spectra. H_2TCNE was also isolated by sublimation. Under rigorously anhydrous conditions, no H_2TCNE was observed, and only a red material (δ 7.5 (s), 1.12 (m)) was observed (vide infra).

Product of $R_3M(TCNE)H$ with TCNE. Isolation of the Red Product. The reactions of the tin, germanium, and silicon hydrides with TCNE under anhydrous conditions all led to an amorphous red material, which showed a characteristic ^1H NMR spectrum consisting of a broad (~40 Hz) resonance at δ 7.5–7.8 ppm. The infrared spectra of materials isolated from each of the metal hydrides are virtually identical, showing absorptions which are characteristic of imine (3120–3340 and 1630–1650 cm^{-1}), alkyl (2840–2920 cm^{-1}), cyanide (2180–2210 cm^{-1}) groups, in addition to others. It can be shown that the red material is not a decomposition product of $Et_3Sn(TCNE)H$, which, when pure, is stable in acetonitrile solutions for prolonged periods. However, the addition of TCNE to this colorless solution rapidly induced the development of the red color, with the concommitant appearance and disappearance of the resonances at δ 7.8 and 3.37 ppm, respectively. Similar highly colored condensation products have been observed in the reactions of the alkyl analogues $R(TCNE)MR_3$ with TCNE.[11]

Potentiometric Titration of Stannane Adduct. A stock solution of 0.06 M sodium hydroxide was standardized with potassium acid phthalate. An acetonitrile solution of $R_3M(TCNE)H$ was deaerated and the titration carried out under an argon atmosphere using a glass and calomel electrode.

Electrochemical Measurements. Electrochemistry was performed on a Princeton Applied Research Model 173 potentiostat equipped with a Model 176 current-to-voltage converter which provided a feedback compensation for ohmic drop between the working and reference electrodes. The voltage follower amplifier (PAR Model 178) was mounted externally to the main potentiostat with a minimum length of high impedance connection to the reference electrode (for low noise pickup). Cyclic voltammograms were recorded on a Houston Series 2000 X-Y recorder. The electrochemical cell was constructed according to the design of Duyne and Reilley.[62] The distance between the platinum working electrode and the tip of the salt bridge was 1 mm to minimize ohmic drop. Bulk coulommetry was carried out in a three-compartment cell of conventional design with a platinum gauze electrode.[63] Complete electrolysis of 0.2 mmol of electroactive material generally required 5–10 min and was graphically recorded on a Leeds and Northrup Speedomax strip chart recorder. The current–time curve was manually integrated.

Kinetics. The reactions were followed spectrophotometrically on a Cary 14 UV spectrophotometer equipped with a thermostated cell compartment regulated at 25 °C. The cell was sealed with a gas-tight rubber septum and deaerated with argon for 15 min prior to each run. The disappearance of the metal hydride was monitored by IR spectroscopy with the aid of a Perkin-Elmer Model 467 grating spectrophotometer. Calibration curves were constructed and shown to obey Beer's law.

Photoinduced Insertion of R_3GeH. Since germanes readily react thermally with TCNE, the photochemical reactions were carried out at very low dilutions, which unfortunately necessitated long irradiation times and obviated quantum yield measurements. For example, separate solutions of 0.0041 M TCNE and 0.014 M Et_3GeH, both in acetonitrile, were mixed at −40 °C and degassed by four successive freeze–pump–thaw cycles and the tubes were sealed under vacuum. Duplicate tubes, one completely wrapped in aluminum foil, were placed side by side in the photochemical apparatus (which allowed the temperature to be maintained at −40 °C with a cold stream of nitrogen) and irradiated through a Pyrex filter with a 250-W tungsten lamp. With this lamp, the Pyrex filter cut off at 320–330 nm (absorbance (wavelength): >2.0 (320), 1.0 (330), 0.5 (340), 0.35 (350), 0.25 (400), 0.25 (500)). At the end of the photolysis, the tubes were immediately stored under liquid nitrogen. The decrease in TCNE concentration was monitored by its absorption spectrum after high dilution to quench the thermal process. In a typical experiment, under conditions in which the thermal control showed no reaction (±1%), the course of the photochemical insertion was as follows: 2.5 h, 5%; 5 h, 9%; 10 h, 16%. The products of the photochemical insertion were examined by ^1H NMR spectroscopy and shown to be the same as those derived thermally (vide supra). The yields based on the product (NMR internal standard method) accorded with those determined from the disappearance of TCNE.

Chemically Induced Dynamic Nuclear Polarization. Since the rate of stannane insertion was too rapid to be controlled and studied, the reaction Et_3GeH was examined at several temperatures between −40 and +4 °C. For example, at 4 °C the insertion occurred with a half-life of 5.2 min under pseudo-first-order conditions. No unusual intensities were observed in the NMR spectra of the reactants or products (vide supra). The reaction between Me_3GeH and TCNE was also examined at several magnetic field strengths (compare studies in ref 13). However, no CIDNP was observed under conditions known to be operative.

Electron Spin Resonance Studies. ESR studies were carried out with a Varian E112 spectrometer equipped with an NMR field marker and a variable-temperature cavity.

The low temperature ESR experiments were carried out as described previously.[13] In a typical experiment, 0.42 M Bu_3GeH and 0.40 M TCNE in a 1:1 mixture of 1,2-dichloropropane and acetonitrile were combined at −78 °C in an ESR tube and degassed by successive freeze–pump–thaw cycles and the tube was sealed. The concentration of the radicals was determined by double integration of the ESR signal relative to a standard diphenylpicrylhydrazyl calibrant. Control experiments showed that no paramagnetic species were formed in the absence of either R_3GeH or TCNE.

Acknowledgment. We thank Dr. Thomas Fehlner for the use of his photoelectron spectrometer and for the measurements of the ionization potentials of Et_3SnH, Et_3GeH, and Et_3SiH, Dr. S. Fukuzumi for help with the ESR experiments, and the National Science Foundation for generous financial support.

References and Notes

(1) For example, see (a) H. O. House, "Modern Synthetic Reactions", 2nd ed., Benjamin, Menlo Park, 1972, Chapter 2; (b) M. N. Rerick in "Reduction", R. L. Augustine, Ed., Marcel Dekker, New York, 1968, p 1.
(2) (a) F. A. Cotton and G. Wilkinson, "Advanced Inorganic Chemistry", 3rd ed., Interscience, New York, 1972, Chapter 23; (b) K. F. Purcell and J. C. Kotz, "Inorganic Chemistry", W. B. Saunders, Philadelphia, 1977, Chapter 17; (c) R. A. Schunn in "Transition Metal Hydrides", E. L. Muetterties, Ed., Marcel Dekker, New York, 1971, p 203.
(3) (a) H. G. Kuivila, *Adv. Organomet. Chem.*, **1**, 47 (1964); *Acc. Chem. Res.*, **1**, 299 (1968). (b) J. J. Zuckerman, *Adv. Chem. Ser.*, **No. 157**, 1 (1976). (c) J. T. Groves and S. Kittisopikul, *Tetrahedron Lett.*, 4291 (1977). (d) J. A. Baritrop and D. Bradbury, *J. Am. Chem. Soc.*, **95**, 5085 (1973).
(4) (a) J. K. Kochi, "Organometallic Mechanisms and Catalysis", Academic Press, New York, 1978, p 501. (b) Compare also H. O. House, *Acc. Chem. Res.*, **9**, 59 (1976).
(5) W. P. Neumann, "The Organic Chemistry of Tin," Wiley, New York, 1970.
(6) E. J. Kupchik in "Organotin Compounds", Vol. 1, A. K. Sawyer, Ed., Marcel Dekker, New York, 1972.

(7) (a) W. P. Neumann, H. Niermann, and R. Sommer, *J. Liebigs Ann. Chem.*, **659**, 27 (1962); (b) W. P. Neumann and R. Sommer, *ibid.*, **675**, 10 (1964); (c) A. J. Leusink and J. G. Noltes, *Tetrahedron Lett.*, 335 (1966); (d) S. Nozakura and S. Konotsune, *Bull. Chem. Soc. Jpn.*, **29**, 322 (1956); (e) L. Goodman, R. M. Silverstein, and A. Benitez, *J. Am. Chem. Soc.*, **79**, 3073 (1957).
(8) L. R. Melby in "The Chemistry of the Cyano Group", Z. Rappoport, Ed., Interscience, New York, 1970, Chapter 10.
(9) H. C. Gardner and J. K. Kochi, *J. Am. Chem. Soc.*, **98**, 2460 (1976).
(10) S. R. Su and A. Wojcicki, *Inorg. Chem.*, **14**, 89 (1975).
(11) H. C. Gardner and J. K. Kochi, *J. Am. Chem. Soc.*, **98**, 558 (1976).
(12) W. J. Middleton, R. E. Heckert, E. L. Little, and C. G. Krespan, *J. Am. Chem. Soc.*, **80**, 2783 (1958).
(13) S. Fukuzumi, K. Mochida, and J. K. Kochi, *J. Am. Chem. Soc.*, **101**, 5961 (1979).
(14) Compare also A. B. Cornwell, P. G. Harrison, and J. A. Richards, *J. Organomet. Chem.*, **140**, 273 (1977).
(15) (a) P. J. Krusic, H. Stoklosa, L. E. Manzer, and P. Meakin, *J. Am. Chem. Soc.*, **97**, 667 (1975); (b) O. A. Reutov, V. L. Rozenberg, V. A. Nikanorov, and G. V. Gavrilova, *Dokl. Akad. Nauk SSSR*, **237**, 690 (1977).
(16) K. S. Chen and N. Hirota in "Techniques of Chemistry", Vol. 6, Part 2, A. Weissberger and G. Hammes, Eds., Wiley, New York, 1973.
(17) (a) M. T. Watts, M. L. Lu, R. C. Chen, and M. P. Eastman, *J. Phys. Chem.*, **77**, 2959 (1973); (b) M. P. Eastman, D. A. Ramirez, C. D. Jaeger, and M. T. Watts, *ibid.*, **80**, 182 (1976); (c) S. Fukuzumi, unpublished results; (d) compare also M. Lehnig, *Tetrahedron Lett.*, 3663 (1977).
(18) E. M. Kosower, "Physical Organic Chemistry", Wiley, New York, 1968, p 293 ff.
(19) C. Reichardt, *Angew. Chem.*, **77**, 30 (1965).
(20) (a) T. P. Fehlner, G. A. Bertram, K. Mochida, and J. K. Kochi, *J. Electron. Spectrosc.*, in press. (b) The value for Ph_3SnH is as yet unmeasured, but, judging from the trends in E° of the couple R_6Sn_2/R_3Sn^+, the value where R = Ph is expected to be considerably smaller than those of the alkyl analogues; see L. Doretti and G. Tagliavini, *J. Organomet. Chem.*, **12**, 203 (1968).
(21) R. S. Taft, Jr., in "Steric Effects in Organic Chemistry", M. S. Newman, Ed., Wiley, New York, 1965, p 597.
(22) J. A. MacPhee, A. Panaye, and J. E. Dubois, *Tetrahedron Lett.*, 3293 (1978).
(23) Compare J. K. Kochi and P. J. Krusic, *Chem. Soc., Spec. Publ.*, **No. 24**, 147 (1970).
(24) R. Foster in "Molecular Complexes", Vol. 2, Crane Russak, New York, 1974, p 107 ff.
(25) R. Foster, "Organic Charge Transfer Complexes", Academic Press, New York, 1969.
(26) R. S. Mulliken and W. B. Person in "Physical Chemistry, An Advanced Treatise," Vol. III, H. Eyring, D. Henderson, and W. Jost, Eds., Academic Press, New York, 1969, p 537.
(27) M. W. Hanna and J. L. Lippert in "Molecular Complexes", Vol. 1, Crane Russak, New York, 1973, p 2 ff.
(28) J. E. Wertz and J. R. Bolton, "Electron Spin Resonance", McGraw-Hill, New York, 1972.
(29) (a) O. W. Webster, W. Mahler, and R. E. Benson, *J. Am. Chem. Soc.*, **84**, 3678 (1962); (b) R. Stösser and M. Siegmund, *J. Prak. Chem.*, **319**, 827 (1977).
(30) (a) The only other important fragment ion ($EtMH_2^+$) is strongly dependent on the ionizing voltage, generally increasing from a minor 5–10% at 20 eV to being the principal ion at 40 eV and above for all metal hydrides. (b) R. G. Cooks, J. H. Beynon, R. M. Caprioli, and G. R. Lester, "Metastable Ions", Elsevier, Amsterdam, 1973.
(31) (a) T. C. Bruice and S. J. Benkovic, "Bioorganic Mechanisms", Vol. 2, Benjamin, New York, 1966, p 343; (b) H. Sund, H. Dieckmann, and K. Wallenfels, *Adv. Enzymol.*, **26**, 115 (1964).
(32) (a) A. K. Colter and M. R. J. Dack in ref 24, p 1 ff. (b) K. Wallenfels, G. Bachmann, H. Dieckmann, K. Friedrich, D. Hofmann, and R. Kern, *Angew. Chem., Int. Ed.*, **3**, 241 (1964); (c) R. H. Abeles, R. F. Hutton, and F. H. Westheimer, *J. Am. Chem. Soc.*, **79**, 712 (1957).
(33) (a) T. Okamoto, A. Ohno, and S. Oka, *J. Chem. Soc., Chem. Commun.*, 181 (1977); (b) A. Ohno and N. Kito, *Chem. Lett.*, 369 (1972); (c) D. C. Dittmer, A. Lombardo, F. H. Batzold, and C. S. Greene, *J. Org. Chem.*, **41**, 2976 (1976); (d) D. J. Creighton, J. Hajdu, G. Mooser, and D. S. Sigman, *J. Am. Chem. Soc.*, **95**, 6855 (1973); (e) J. Hajdu and D. S. Sigman, *ibid.*, **98**, 6060 (1976); (f) C. O. Schmakel, K. S. V. Santhanam, and P. J. Elving, *ibid.*, **97**, 5083 (1975).
(34) K. Schellenberg in "Pyridine Nucleotide Dependent Dehydrogenases", H. Sund, Ed., Springer Verlag, Berlin, 1970, p 15.
(35) R. J. Kill and D. A. Widdowson, *J. Chem. Soc., Chem. Commun.*, 755 (1976); J. J. Steffens and D. M. Chipman, *J. Am. Chem. Soc.*, **93**, 6694 (1971).
(36) R. C. Poller, "The Chemistry of Organotin Compounds", Academic Press, New York, 1970.
(37) (a) D. J. Carlsson and K. U. Ingold, *J. Am. Chem. Soc.*, **90**, 7047 (1968); (b) see, however, S. Kozuka and E. S. Lewis, *ibid.*, **98**, 2254 (1976).
(38) It is not demanded, however, since the formation constants K_{CT} are generally small, and it is possible that the charge-transfer complex represents only an unrelated side product.
(39) Compare T. H. Lowry and K. S. Richardson, "Mechanism and Theory in Organic Chemistry", Harper and Row, New York, 1976, p 99 ff.
(40) R. S. Taft, Jr., in "Steric Effects in Organic Chemistry", M. S. Newman, Ed., Wiley, New York, 1965, p 587 ff.
(41) C. L. Wong, K. Mochida, A. Gin, M. A. Weiner, and J. K. Kochi, *J. Org. Chem.*, in press.
(42) N. Sutin in "Inorganic Biochemistry", Vol. 2, G. L. Eichhorn, Ed., Elsevier, Amsterdam, 1973, p 611.
(43) W. L. Reynolds and R. W. Lumry, "Mechanisms of Electron Transfer", Ronald Press, New York, 1966.
(44) The same figure applies to charge transfer of R_4M and TCNE (see ref 13).
(45) The transience of this radical pair contrasts with the persistence of the analogous ethyl TCNE radical pair ($Et{\cdot}Et_3Ge^+TCNE^{-\cdot}$) derived from tetraethylgermane and TCNE under the same conditions as those described in ref 13.
(46) S. Fukuzumi, unpublished observations.
(47) A similar observation was made in the analogous electron-transfer process with R_4M and TCNE (see ref 13).
(48) Thus, the predominance of the fragment ion, Et_2MH^+ over Et_3M^+ by a factor of >10 in eq 18 and 19, suggests that loss of ethyl is favored over loss of hydrogen. This selectivity is opposed to the observation of TCNE insertion exclusively into the M–H bond and the absence of any isomeric adducts resulting from insertion into an alkyl–metal bond.
(49) (a) An equivalent, experimentally indistinguishable alternative is that the first-formed ion pair derived by ionization from the HOMO involving the alkyl–metal σ-bonding orbital rapidly relaxes to a new ion pair equivalent to that derived by excitation of the hydrido-metal orbital. (b) Taken further, this argument suggests that steric size is the important distinguishing feature in the comparative reactivity of hydrido and alkyl ligands.
(50) (a) A. K. Colter, G. Saito, and F. J. Sharom, *Can. J. Chem.*, **55**, 2741 (1977); (b) A. K. Colter, G. Saito, F. J. Sharom, and A. P. Hong, *J. Am. Chem. Soc.*, **98**, 7833 (1976); (c) compare also G. Saito and A. K. Colter, *Tetrahedron Lett.*, 3325 (1977).
(51) (a) W. A. Pryor and K. G. Kniepp, *J. Am. Chem. Soc.*, **93**, 5584 (1971); (b) E. S. Lewis and M. M. Butler, *J. Chem. Soc., Chem. Commun.*, 941 (1971).
(52) E. S. Lewis and M. M. Butler, *J. Am. Chem. Soc.*, **98**, 2257 (1976).
(53) (a) E. S. Lewis and K. Ogino, *J. Am. Chem. Soc.*, **98**, 2260 (1976); (b) E. S. Lewis and E. C. Nieh, *ibid.*, **98**, 2268 (1976).
(54) E. S. Lewis and K. Ogino, *J. Am. Chem. Soc.*, **98**, 2264 (1976).
(55) (a) F. H. Westheimer, *Chem. Rev.*, **61**, 265 (1961); (b) L. Melander, "Isotope Effects on Reaction Rates", Ronald Press, New York, 1960.
(56) (a) The ionization potentials of metal deuterides have not been resolved from those of metal hydrides owing to limitations in resolution: H. Bock, private communication. No difference is expected in the vertical ionization energies of protio and deuterio compounds under conditions where the Born–Oppenheimer approximation applies. Similarly, the adiabatic ionization energies are expected to change only somewhat as a result of the changes in the Franck–Condon profiles, but only marginally: E. Heilbronner, private communication. (b) The isotope effect in the photoelectron spectra of HF and DF is unresolved (J. W. Rabalais, "Principles of Ultraviolet Photoelectron Spectroscopy", Wiley, New York, 1977, p 65). Compare also the isotope effects in the PES of alkanes (S. G. Lias, P. Ausloos, and Z. Horvath, *Int. J. Chem. Kinet.*, **8**, 725 (1976)).
(57) (a) W. A. Pryor and W. H. Hendrickson, Jr., *J. Am. Chem. Soc.*, **97**, 1582 (1975); (b) See also W. A. Pryor, *ACS Symp. Ser.*, **No. 69**, 33 (1978).
(58) R. K. Ingham, S. D. Rosenberg, and H. Gilman, *Chem. Rev.*, **60**, 459 (1960).
(59) (a) O. H. Johnson, *Chem. Rev.*, **48**, 259 (1951). (b) Compare also D. Quane and R. S. Bottei, *ibid.*, **63**, 403 (1963); C. Eaborn "Organosilicon Compounds", Butterworths, London, 1960.
(60) P. D. George and J. R. Ladd, *J. Org. Chem.*, **27**, 340 (1962).
(61) E. R. Birham and P. H. Javora, *Inorg. Synth.*, **12**, 53 (1970).
(62) R. P. Van Duyne and C. N. Reilley, *Anal. Chem.*, **44**, 142 (1972).
(63) J. F. O'Donnell, J. T. Ayres, and C. K. Mann, *Anal. Chem.*, **37**, 1161 (1965).